direction of a cylindrical vehicle, the possibility of implementation of the d. c. magnetic fields was tacitly assumed. However, in practice, one does not find such ideal models. Moreover, the problem of generation of a d. c. magnetic field efficiently in an appropriate orientation may pose a stumbling block to the whole approach. Therefore, first of all we shall show that at least in principle a d. c. magnetic field in the angular direction of a cylindrical geometry is possible. Once this principle is accepted, then the second major step will be how to generate this magnetic field more efficiently in a laboratory or in an actual space vehicle.

Consider a loop of a coil carrying a d. c. current inside a cylindrical space vehicle, such that both sides of the coil are not too close to the axis of the cylinder, as shown in Fig. 1c. Because of this particular choice[6] of geometry of the coil carrying a current, the generated d. c. (static) magnetic field will have both radial and the angular components which are also functions of ρ and ϕ. The angular fields will be stronger at points such as A and B in Fig. 1c. Now, if the region A or B containing the strongest angular magnetic field is large enough in comparison with the wavelength and the size of the circumferential radiating source (slot antenna which does not cover the entire angular region 0 to 2π) which should be located on the surface of the vehicle near A or B, this situation may be considered reasonably close to the ideal case discussed in the analysis. It is anticipated that such a situation can be created in a laboratory, possibly with a little effort. One can easily see that the generation of a static magnetic field in the axial direction of a cylinder is also not very difficult, at least in a laboratory.

If in the near future, the development of very powerful electromagnets with reasonable size can be achieved, then the implementation of a static magnetic field in the angular direction of a conical or a cylindrical vehicle or in the axial direction of a cylindrical vehicle will be more practical. For practical purposes, the gap between the two pole pieces of the magnet should be large enough to include the radiating element.

Conclusion

In concluding this work, it would seem that the problem of the blackout of radio communications due to a plasma sheath can be at least eliminated in principle by a static magnetic field. Practical application of the theory requires a static magnetic-field, appropriately generated, which does not add appreciable weight to the present antenna and transmitter configuration. Further work should include such a laboratory study. It is hoped that developments of strong electromagnets using superconductors might play an important role in the problem of the radio communication blackout during reentry. The analysis presented is appropriate for the simplified models considered here. An analysis may not be developed for an actual complicated re-entry situation. However, the simple approach made here tells us, at least, in what way the future work may be directed.

It is important to note that in all the foregoing examples, the orientation of the antenna and the static magnetic field is chosen in such a way that the field components are independent of the component of the dielectric tensor parallel to the static magnetic field. This choice enables one to control more effectively the electromagnetic waves by controlling the applied d. c. magnetic field.

References

[1] Rotman, W. and Meltz, G., (eds.), *Electromagnetic Effects of Re-Entry* (Pergamon Press, New York, 1961).

[2] Hodara, H., "The use of magnetic fields in the elimination of the re-entry radio blackout," Proc. Inst. Radio Engrs. **49**, 1827–1830 (December 1961).

[3] Siegel, K. M. and Alperin, H. A., "Scattering by a cone," Radiation Lab., Univ. of Michigan, Rept. UMM-87 (January 1952).

[4] Felsen, L. B., "Radiation from source distributions on cones and wedges," Research Rept. R-574-57, P.I.B.-502, Microwave Research Inst., Polytechnic Institute of Brooklyn, N.Y. (1957).

[5] Samaddar, S. N., "Two-dimensional diffraction in homogeneous anisotropic media," Inst. Radio Engrs. Trans. **AP-10** (September 1962); see problem #B-3.

[6] Weber, E., *Electromagnetic Fields—Theory and Application* (John Wiley & Sons, Inc., New York, 1950), Vol. 1, p. 136.

Large Displacement Analysis of Axially Compressed Circular Cylindrical Shells

C. H. Tsao*
Aerospace Corporation, El Segundo, Calif.

Nomenclature

A_{11}, A_{19}, A_{91}	=	functions of wavelength ratio
E	=	modulus of elasticity
L	=	shell length
R	=	mean shell radius
W	=	potential energy
W_1, W_2, W_3	=	extensional strain energy, bending strain energy, potential of applied axial load, respectively
a, b, e	=	deflection parameters
t	=	wall thickness
u, v, w	=	axial, circumferential, and radial displacements, respectively, at an arbitrary point
$\bar{u}$, $\bar{v}$, $\bar{w}$	=	axial, circumferential, and radial displacements, respectively, on median surface of shell
x	=	axial coordinate
z	=	radial coordinate
$\gamma_{x\phi}$, ϵ_x, ϵ_ϕ	=	shear and normal strains at an arbitrary point
$\bar{\gamma}_{x\phi}$, $\bar{\epsilon}_x$, $\bar{\epsilon}_\phi$	=	shear, axial, and circumferential strains on median surface of shell, respectively
ϵ	=	unit end shortening
η	=	$\pi^2 Rt/\lambda_\phi^2$
λ_x, λ_ϕ	=	axial and circumferential half wavelengths, respectively
μ	=	λ_ϕ/λ_x
ν	=	Poisson's ratio (0.3)
ν_{11}, ν_{22}, ν_{12}	=	functions of $\bar{u}$, $\bar{v}$, $\bar{w}$
ξ	=	deflection parameter
σ	=	applied average axial compressive stress
ϕ	=	circumferential coordinate
χ_{11}, χ_{22}, χ_{12}	=	functions of $\bar{u}$, $\bar{v}$, $\bar{w}$
ω	=	$\xi\eta$

Introduction

BY use of a large displacement analysis it was shown in Refs. 1–3 that buckled equilibrium configurations exist at loads considerably below the classical buckling load. In these analyses, only nonlinear terms involving the radial displacement w were included. The present note contains an investigation of the influence of the further retention of nonlinear terms involving the axial and circumferential displacements u and v on the minimum equilibrium load in the post-buckling range.

Analysis

Strain-displacement relations for the general shell derived from nonlinear theory of elasticity and Kirchhoff's assumption are given in Ref. 4 and modified in Ref. 5. These can be

Received April 13, 1964; revision received August 10, 1964. This research was supported by the U. S. Air Force under Contract No. AF 04(695)-269.

* Head, Stress Analysis Section, Aerodynamics and Propulsion Research Laboratory. Member AIAA.

Table 1 Minimum $\sigma R/Et$ for various values of t/R

t/R	a	b	η	μ	ω	$\sigma R/Et$	$\epsilon R/t$
0	0.1860	0.0741	0.2269	0.390	1.429	0.1824	0.4009
0.002	0.1832	0.0748	0.2301	0.390	1.430	0.1802	0.3946
0.01	0.1802	0.0793	0.3067	0.460	1.419	0.1802	0.3990
0.03	0.1742	0.0982	0.3896	0.570	1.396	0.1906	0.4430

readily specialized to the cylindrical shell shown in Fig. 1 to give

$$\left.\begin{aligned} \epsilon_x &= \bar{\epsilon}_x + z\chi_{11} + z^2\nu_{11} \\ \epsilon_\phi &= \bar{\epsilon}_\phi + z\chi_{22} + z^2\nu_{22} \\ \gamma_{x\phi} &= \bar{\gamma}_{x\phi} + z\chi_{12} + z^2\nu_{12} \end{aligned}\right\} \tag{1}$$

where

$$\bar{\epsilon}_x = \frac{\partial \bar{u}}{\partial x} + \frac{1}{2}\left[\left(\frac{\partial \bar{u}}{\partial x}\right)^2 + \left(\frac{\partial \bar{v}}{\partial x}\right)^2 + \left(\frac{\partial \bar{w}}{\partial x}\right)^2\right]$$

$$\bar{\epsilon}_\phi = \ldots, \text{ etc.}$$

Nonlinear terms of $\bar{u}$, $\bar{v}$, as well as $\bar{w}$ have been retained in the preceding expressions. The potential energy of the axially compressed shell is given by

$$W = \int_0^L \int_0^{2\pi} \int_{-t/2}^{t/2} \frac{E}{4(1-\nu^2)} \times [2(\epsilon_x + \epsilon_\phi)^2 + (1-\nu)(\gamma_{x\phi}^2 - 4\epsilon_x\epsilon_\phi)] \times R\,dx\,d\phi\,dz - 2\pi Rt\sigma \int_0^L \left(\frac{\partial \bar{u}}{\partial x}\right) dx \tag{2}$$

In the derivation of the preceding formulas, only the deformations have been assumed to be small. The displacements $\bar{u}$, $\bar{v}$, as well as $\bar{w}$ are arbitrary and may be large. The assumed expressions for the deflection functions $\bar{u}$, $\bar{v}$, and $\bar{w}$ will be the same as Kempner's in Ref. 2. These are obtained by neglecting higher orders of $\bar{u}$, $\bar{v}$ and their derivatives in the basic equations. Thus,

$$\bar{w} = -\xi t\left(\cos\frac{\pi x}{\lambda_x}\cos\frac{\pi R\phi}{\lambda_\phi} + a\cos\frac{2\pi x}{\lambda_x} + b\cos\frac{2\pi R\phi}{\lambda_\phi} + e\right)$$
$$\bar{u} = \ldots \tag{3}$$
$$\bar{v} = \ldots$$

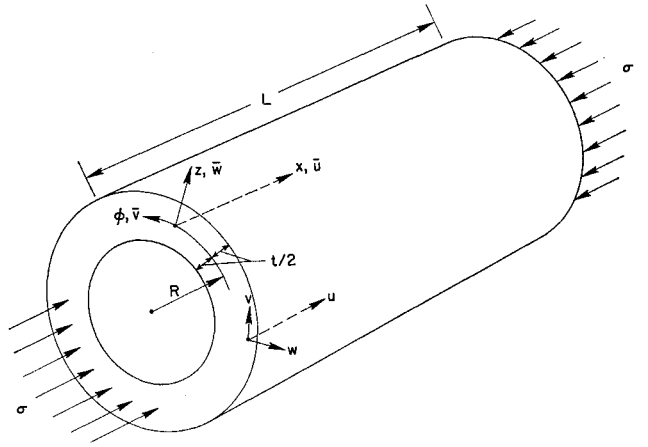

Fig. 1 Coordinates and components of displacements of axially compressed circular cylindrical shell.

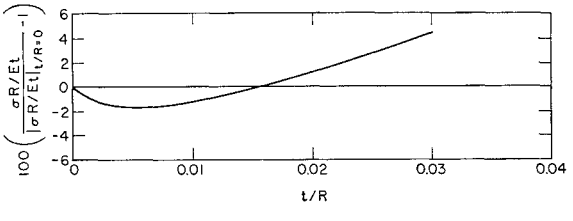

Fig. 2 Percent difference between $\sigma R/Et$ and $\sigma R/Et$ at $t/R = 0$.

With the help of Eqs. (1) and (3), Eq. (2) can be integrated to give

$$W = W_1 + W_2 + W_3 \tag{4}$$

where

$$\left(\frac{R}{\pi Et^3L}\right) W_1 = \frac{\omega^2}{\eta^2}\left[\omega^2\left\{A_{11}[(a+b)^2 + 4a^2b^2] + A_{19}a^2 + A_{91}b^2 + \frac{\mu^4}{128}\right\} + A_{11}\left[\frac{1}{4} - \omega(a+b)\right] + \frac{1}{128}(\omega - 8a)^2\right] + \left(\frac{\sigma R}{Et}\right)^2 - \frac{t}{R}\frac{\omega^2}{\eta^2}\left\{\frac{A_{11}\omega^2}{2\eta}\left(a - \frac{\omega}{8}\right) \times [2\omega(a+b) - 1] + \frac{\omega}{\eta}\left(3A_{19}\omega a^2 + \frac{\omega - 8a}{32} + \frac{\mu^4\omega}{64}\right) + \frac{\mu^2}{4}\cdot\frac{\sigma R}{Et}\right\} + \left(\frac{t}{R}\right)^2\left[\frac{\omega^4}{64\eta^4(1-\nu^2)}\right]\left(9 - 18b\omega - \frac{\omega^2}{4}\right) - \left(\frac{t}{R}\right)^3\left[\frac{9\omega^4}{64\eta^5(1-\nu^2)}\right]$$

$$\left(\frac{R}{\pi Et^3L}\right) W_2 = \frac{\omega^2}{48(1-\nu^2)} \times [(1+\mu^2)^2 + 32(\mu^4a^2 + b^2)] - \frac{t}{R}\left[\frac{\omega^2(1+\mu^2)}{24\eta(1-\nu^2)}\right]$$

$$\left(\frac{R}{\pi Et^3L}\right) W_3 = -2\frac{\sigma R}{Et}\left[\frac{\sigma R}{Et} + \frac{\omega^2\mu^2}{8\eta}(1 + 8a^2)\right]$$

$$A_{11} = \frac{\mu^4}{(1+\mu^2)^2} \qquad A_{19} = \frac{\mu^4}{(1+9\mu^2)^2}$$

$$A_{91} = \frac{\mu^4}{(9+\mu^2)^2}$$

The preceding expressions of W are precisely those given in Ref. 2 plus a few terms involving t/R. These t/R terms therefore represent the correction terms due to the inclusion of nonlinear terms of $\bar{u}$, $\bar{v}$ in the basic shell equations. In Eq. (4), a number of correction terms have already been discarded and do not appear. In order to decide which correction terms to retain and which ones to discard, the uncorrected strain energy $(R/\pi Et^3L)(W_1 + W_2)$ is computed from Eqs. (24) and (25) of Ref. 2 at $\sigma R/Et = 0.182$, $a = 0.186$, $b = 0.074$, $\eta = 0.227$, $\mu = 0.390$, and $\omega = 1.429$. For the previous values of $\sigma R/Et$, a, b, η, μ, and ω, and for $t/R \leq 0.02$, correction terms that are numerically less than 2% of the preceding uncorrected $(R/\pi Et^3L)(W_1 + W_2)$ are discarded. The condition of stationary potential energy is now imposed by setting to zero the partial derivatives of W with respect to a, b, η, μ, and ω, respectively, for constant σ. Five equations are obtained which can be solved for the five unknowns a, b, η, μ, and ω.

Numerical Solution

Poisson's ratio ν has been assumed to be 0.3 throughout the numerical computations. For $t/R \to 0$, the five equations on a, b, η, μ, and ω become identical to the corresponding equations in Ref. 2. The present computer solution of these five equations agrees with the solution given in Ref. 2, except in the value for μ. In Ref. 2, the value of μ at minimum postbuckling load is given as 0.362, whereas the present com-

puter solution gives 0.390. For other values of t/R, the minimum $\sigma R/Et$ and the corresponding values of a, b, η, μ, ω, and $\epsilon R/t$ are given in Table 1. It is seen that the minimum $\sigma R/Et$ now depends on t/R, whereas in Ref. 2 this dependency does not exist. The influence of t/R on $\sigma R/Et$ is shown in Fig. 2. For $t/R = 0.03$, the minimum $\sigma R/Et$ has a 4.5% increase over that at $t/R = 0$.

References

[1] von Kármán, T. and Tsien, H.-S., "The buckling of thin cylindrical shells under axial compression," J. Aeronaut. Sci. **8**, 303 (1941).

[2] Kempner, J., "Postbuckling behavior of axially compressed circular cylindrical shells," J. Aeronaut. Sci. **17**, 329–342 (1954).

[3] Almroth, B. O., "Postbuckling behavior of axially compressed circular cylinders," AIAA J. **1**, 630 (1963).

[4] Novozihilov, V. V., *Foundations of the Nonlinear Theory of Elasticity* (Graylock Press, Rochester, N. Y., 1953), pp. 186–193.

[5] Tsao, C. H., "Strain-displacement relations in large displacement theory of shells," AIAA J. **2**, 2060–2062 (1964).

Shock Shape Generalization for Inverse Blunt Body Methods

RICHARD A. BATCHELDER*

Douglas Aircraft Company, Santa Monica, Calif.

THE purpose of this note is to set forth a concept and technique for generalizing shock wave geometries while maintaining the feature of equal spacing between finite difference points in determinate form. This concept is useful to the solution of inviscid flow fields around blunt noses in supersonic or hypersonic flight, particularly in the case of the inverse or shock-initiated approach.

In essence, the inverse blunt-body approach starts with an assumed shock shape and applies finite difference techniques to the equations of motion (conservation of mass, momentum, and energy), marching progressively inward from the shock wave to the body. The body contour itself is established by this process, and is hoped to be close to a specified contour of practical interest. In many cases, particularly when the desired body contour is circular, the bodies attainable from simple shock shapes are close enough to the desired contour for some engineering purposes. However, there occur at least two situations in which more general shock shapes are needed: a) when greater accuracy in body contour matching is desired for more refined predictions of local properties; and b) when simple shock shapes fail to provide data sufficiently far around the body to adequately envelop the sonic line and supply direct input lines for method of characteristics programs.

Generalization from simple shock shapes to a family of conic section shock shapes was achieved by Van Dyke,[1] using a special orthogonal coordinate system. The program of Refs. 2 and 3 contains a one-parameter capability for modifying shock shapes from basic conic section shock geometries. These are significant steps in the direction of shock shape generalization.

The finite-difference processes customarily applied involve the numerical differentiation of flow properties along the shock wave (or, subsequently, along lines displaced therefrom across known finite steps). The numerical difference formulas that are most efficiently applicable require that the data points at which properties are known be equally spaced with respect to some spacing parameter, usually one of the coordinates in some geometric coordinate system. The reference circle coordinate system of Ref. 4 (Fig. 1 herein), somewhat independent of shock shape, uses the reference circle arc length (or radial angle) as a spacing parameter applied through the difference formulas of Ref. 5.

Received May 11, 1964; revision received September 14, 1964. This paper was prepared under the sponsorship of the Douglas Aircraft Company Independent Research and Development Program.

* Design Specialist, Solid and Fluid Physics Department, Missile and Space Systems Division. Member AIAA.

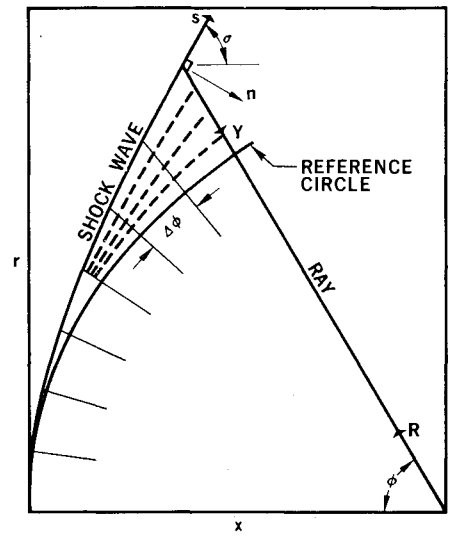

Fig. 1 Reference circle system.

Reference Circle Method Geometric Development

The reference circle concept of Ref. 4 was developed to provide an axis system somewhat independent of shock shape, capable of scale changes, and applicable to cases in which shock arc lengths are not easily determined. The simplest and most limited application of the reference circle method is to let the shock wave coincide with the reference circle, in which case the curvilinear equations of motion with basic variables of P, ρ, u, and v (Refs. 4 and 6) can be applied without any geometric adjustments.

Next in order of difficulty is the operation of the reference circle system initiated from a simple analytic, noncircular shock shape. The geometric consequences of this advance are portrayed in Fig. 1. The objective is to march from the shock wave to the body along rays of constant ϕ, spaced apart by constant intervals $\Delta\phi$. Once the reference circle is reached, the process is identical to that behind a circular shock wave. Operations in the front-end region will now be discussed.

First of all, the intersections of the rays with the shock wave are determined. An exact analytic solution for these intersections with conic section shock shapes is presented in Ref. 4; a convergent iterative solution for catenary geometry is also given.

The determination of the (x, r) coordinates at all shock-ray intersections leads immediately to the local geometric slopes at each point dr/dx. These could often be found as exact analytic expressions; however, for the purpose of generality, they are found through the difference formulas as $(dr/d\phi)/(dx/d\phi)$. The local shock angles, $\sigma = \tan^{-1}(dr/dx)$, together with given conditions in front of the shock wave, determine conditions immediately behind the shock wave at each local point. Another useful geometric parameter found with the aid of the difference formulas is

$$ds/d\phi = [R^2 + (dR/d\phi)^2]^{1/2} \quad (1)$$

The shockwise derivatives are then simply

$$df/ds = (df/d\phi)/(ds/d\phi) \quad (2)$$

where f is any property or velocity component (P, ρ, V_n, V_s).